Letter

Magnetic ground state of NdB_4: Interplay between anisotropic exchange interactions and hidden order on a Shastry-Sutherland lattice

D. D. Khalyavin,[1] D. Brunt,[2,3] N. Qureshi,[4] A. R. Wildes,[4] B. Ouladdiaf,[4] R. D. Johnson,[5] G. Balakrishnan,[3] and O. A. Petrenko[3]

[1]*ISIS Facility, STFC Rutherford Appleton Laboratory, Chilton, Didcot, OX11 0QX, United Kingdom*

[2]*National Physical Laboratory, Hampton Road, Teddington TW11 0LW, United Kingdom*

[3]*Department of Physics, University of Warwick, Coventry CV4 7AL, United Kingdom*

[4]*Institut Laue-Langevin, 71 avenue des Martyrs, CS 20156, 38042 Grenoble Cedex 9, France*

[5]*Department of Physics and Astronomy, University College London, Gower Street, London, WC1E 6BT, United Kingdom*

(Received 22 September 2023; accepted 22 May 2024; published 24 June 2024)

The neodymium tetraboride NdB_4, crystalizing into a tetragonal crystal structure, has the magnetic ions located on a Shastry-Sutherland lattice. The compound undergoes several magnetic phase transitions and exhibits a complex multi-k ground state that has so far been elusive. Here we report the solution and quantitative refinement of the magnetic ground state of NdB_4 based on neutron diffraction data. The magnetic structure consists of two separate components; one of them is confined within the ab plane and makes an orthogonal all-in-all-out spin configuration maintaining translation symmetry of the crystal. Another is pointing along the c axis, and this component forms an anharmonic spin density wave consisting of three-up-two-down sequences with fivefold periodicity. The in-plane and out of plane spin structures represent distinct magnetic instabilities which normally would not coexist. Their simultaneous presence in the same phase is an interesting phenomenon associated with anisotropic exchange interactions and coupling to a symmetry breaking nonmagnetic order parameter undetectable by the available diffraction data.

DOI: 10.1103/PhysRevB.109.L220411

The Shastry-Sutherland model (SSM), introduced as a theoretical concept of a frustrated antiferromagnet with an exactly solvable ground state [1], has been at the forefront of contemporary magnetism for several decades. $SrCu_2(BO_3)_2$ (SCBO), the only well established realisation of the quantum SSM, provided a plethora of the unconventional phenomena, including fractional magnetization [2] and discontinuous quantum phase transitions [3,4]. A quantum magnetic analog to the critical point of water has been suggested to exist on the phase diagram of SCBO [5]. The latest discovery is a suggestion for the existence of the long-sought deconfined quantum critical point [6].

It has long been recognized that competing magnetic interactions might give rise to a broad range of exotic ground states not only in quantum but also in classical spin systems. The best-known example being spin ice materials in which strong local magnetic anisotropy combined with the frustrated triangular topology results in highly degenerate two-in-two-out ground states with associated magnetic monopole physics [7]. The search for experimental realizations of the SSM for classical spins has not yet returned many candidates [8], as the required exchange topology is not trivial—a square planar lattice, where only half of square plaquettes have a single next nearest neighbor interaction J_2 [1]. The key parameter for the SSM is the J_1/J_2, ratio between nearest and next nearest neighbor interactions.

The rare-earth (R) tetraborides family members RB_4 could be considered the closest approximation to the SSM. The RB_4 compounds possess complex noncollinear magnetic structures and exhibit successive magnetic phase transitions and plateaus at fractional values of the saturation magnetization [9–13]. In particular, orthogonal patterns of the in-plane magnetic component (m_{xy}) were found in the ground state of the $R =$ Nd, Gd, Tb, Dy, and Ho compounds [14–18]. These patterns are characterized by a $\mathbf{k}_1 = 0$ propagation vector, and in the case of Nd, Dy, and Ho, the in-plane configurations coexist with ordered out-of-plane components (m_z).

The magnetic ground states of ErB_4 and TmB_4 were reported to be collinear with moments polarized along the c axis [19,20]. A particular interest was generated by DyB_4 exhibiting a low-temperature monoclinic structural distortion attributed to quadrupolar order [21–23]. The transition takes place below the long-range magnetic ordering of the z component of Dy moments, and triggers the onset of in-plane magnetic order where the m_{xy} components of the Dy moments are ordered along the orthogonal [110] and [1$\bar{1}$0] directions. The presence of quadrupolar order has also been suggested for Ho and Nd compounds [14], but no associated structural distortions were detected. The latter compound exhibits three distinct magnetic phases with apparently the most complex ground state magnetic structure of the whole series. The structure was reported to involve $\mathbf{k}_1 = 0$ in-plane (m_{xy}^{k1}) and out-of-plane (m_z^{k1}) ordered Fourier components, each with distinct symmetries, coexisting with multi-k incommensurate

order [14,15]. In spite of the several extensive studies of the magnetic order in NdB_4, no quantitative magnetic structure refinement has been achieved so far. A quantitative determination of the ground state is however a key ingredient to obtain a comprehensive understanding of the competing exchange interactions in this material as well as in the whole series of rare earth tetraborides.

Here we report the full magnetic structure solution for the ground state of NdB_4 using single crystal and powder neutron diffraction. An extension of the two-dimensional (2D) SSM into the third direction and inclusion of an additional in-plane interaction is required to properly model NdB_4. The resulting structure consists of an orthogonal all-in-all-out ordering of the m_{xy} component of the Nd moments and an anharmonic spin density wave in m_z, locked to a commensurate value of the propagation vector and resulting in three-up-two-down sequences. This exotic ground state reveals the presence of a nonmagnetic order parameter, not directly detectable in the present diffraction experiment. This nonmagnetic order parameter mediates a coupling between the in-plane and out-of-plane magnetic components by creating a staggered internal field.

NdB_4 crystals, using isotopically enriched boron (99% ^{11}B), were grown and characterized as described in a recent publication [24]. To ensure the highest purity possible, single crystal samples were ground to a fine powder and used for polycrystalline measurements. Single crystal polarized neutron diffraction experiments, with the polarization normal to the scattering plane, were carried out using the D7 instrument at the Institut Laue-Langevin, Grenoble, France [25]. The sample (2.4 g) was fixed to an aluminium strip defining the horizontal $(h0l)$ scattering plane. A wavelength of 4.8 Å was used and scans were made by rotating the sample in 1° increments around the vertical axis at temperatures of 30, 12, and 1.5 K.

Powder neutron diffraction data were collected at the ISIS Neutron and Muon Facility of the Rutherford Appleton Laboratory (UK), on the WISH diffractometer [26]. The sample (∼1 g) was loaded into a cylindrical 3 mm diameter vanadium can and measured in the temperature range of 1.5–25 K using an Oxford Instrument Cryostat. Rietveld refinements of the crystal and magnetic structures were performed using the FullProf program [27] against the data measured in detector banks at average 2θ values of 58°, 90°, 122°, and 154°, each covering 32° of the scattering plane.

The paramagnetic powder neutron diffraction data collected at $T = 25$ K could be refined using the tetragonal $P4/mbm$ model with Nd at the $4g$ Wyckoff position. The data also revealed a cubic NdB_6 impurity phase, which was included into the refinement procedure and did not compromise the obtained structural information (see Fig. S1 of the Supplemental Material [28]). No changes in the crystal structure were detected down to the lowest measured temperature of 1.5 K. The lower temperature diffraction patterns also contained sets of magnetic reflections, which could be isolated by subtracting the paramagnetic data (see Fig. S2 of the Supplemental Material [28]). By inspecting the temperature behavior of the magnetic reflections, one could identify three distinct magnetic phases. The high-temperature phase is stable in the range of $T_{N2} = 6.8$ K to $T_{N1} = 17$ K, intermediate phase

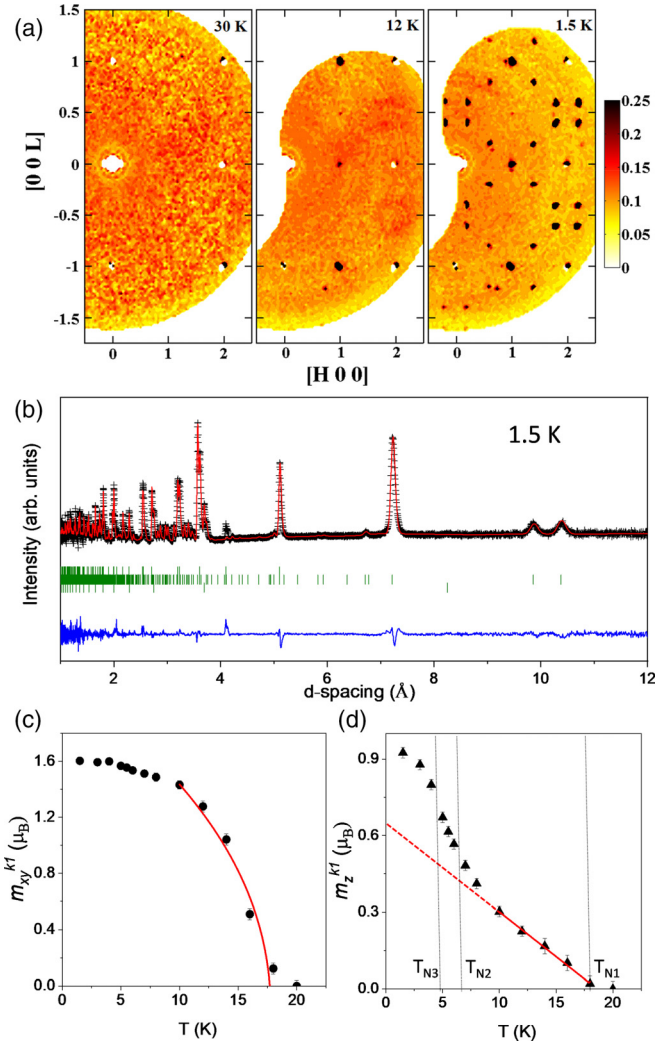

FIG. 1. (a) Spin-flip single crystal neutron diffraction intensity maps of $(h0l)$ plane measured on the D7 instrument. (b) Rietveld refinement of the powder neutron diffraction data collected on the WISH instrument. The pattern contains only magnetic intensities obtained by subtraction between the low-temperature (1.5 K) and the high-temperature (25 K) data. (c) Temperature dependence of the in-plane Fourier component, m_{xy}^{k1}. The red line is a power law fit with the critical exponent 1/2. (d) Temperature dependence of the out-of-plane Fourier component, m_z^{k1}. The red line is a power law fit with the critical exponent one.

between $T_{N3} = 4.9$ K and $T_{N2} = 6.8$ K, and the ground state phase sets in below $T_{N3} = 4.9$ K, in good agreement with the bulk properties measurements on the same samples [29,30] as well as previous reports from different groups [14,15].

We used the single crystal polarized neutron scattering data [Fig. 1(a)] to index the powder diffraction patterns, which were then implemented into quantitative refinement of the magnetic structure. The single crystal measurements were restricted to a single reciprocal plane which was not sufficient for the quantitative analysis. Concurring with the single crystal polarized neutron scattering data, the powder diffraction pattern collected at 1.5 K could be indexed using three magnetic propagation vectors $\mathbf{k}_1 = 0$, $\mathbf{k}_2 = (1/5, 0, -2/5)$, and $\mathbf{k}_3 = 2\mathbf{k}_2 = (2/5, 0, -4/5)$. The refinement of the Fourier

components based on our high-resolution data confirmed their commensurate nature and the relation between $\mathbf{k}_2$ and $\mathbf{k}_3$. Note the previous single crystal studies [14,15] reported only $\mathbf{k}_1$ and $\mathbf{k}_2$ in the ground state, presumably due to the limited portion of accessible reciprocal space. The commensurate nature of the modulation and the presence of the second harmonic are the key experimental observations needed to appreciate the magnetic structure solution.

A generally accepted proposition is that even magnetic harmonics in modulated structures are forbidden by time reversal symmetry unless an external magnetic field is applied. The field-induced components are translationally invariant and can give rise to new even power free-energy terms that respect time reversal symmetry. Such field-induced even harmonics typically cause the modulation to lock into a commensurate propagation vector to form constant moment structures with an unequal number of spins along the field (up, U) and opposite to it (down, D). These structures generate a significant net magnetization along the field due to the imbalance between U and D spins, hence optimizing the Zeeman coupling term. A cascade of uncompensated, commensurate up and down field-induced magnetic structures has been recently reported by Amorese *et al.* [31] in $CeRh_3Si_2$. Another example is the two-up-one-down spin configuration stabilized by magnetic field in many triangular frustrated systems [32]. In diffraction, the characteristic signature of these constant moment structures is the presence of higher-order even harmonics. Our approach to solve the ground state magnetic structure of NdB_4 was based on this logic, where the translationally invariant $\mathbf{k}_1 = 0$ Fourier component played the role of an internal field, defining the nominal up and down directions that alternate in the crystal. The obtained magnetic structure involves ordering of the in-plane m_{xy} projections of the Nd magnetic moments, polarized either along the [110] or [1$\bar{1}$0] directions and forming an orthogonal all-in-all-out configuration with $\mathbf{k}_1 = 0$ propagation vector [Fig. 2(a)]. In addition, the out-of-plane m_z projection of the moments are ordered in a three-up-two-down structure with fivefold periodicity along a and c. This commensurate spin density wave consists of three Fourier components with $\mathbf{k}_1 = 0$ (m_z^{k1}), $\mathbf{k}_2 = (1/5, 0, -2/5)$ (m_z^{k2}), and $\mathbf{k}_3 = 2\mathbf{k}_2 = (2/5, 0, -4/5)$ (m_z^{k3}). The m_z^{k1} component represents ferromagnetic bc planes antiferromagnetically coupled along the a axis [Fig. 2(b)], implying the staggered character of the internal field. The net magnetization generated by the three-up-two-down structure also alternates in the same manner. Considering three-up-two-down spin configurations, two distinct sequences of the up and down spins can be distinguished: UUUDD and UUDUD. In NdB_4, a model in which UUUDD and UUDUD sequences propagated along the a and c axes, respectively [Fig. 2(c)], provided an excellent fit to the neutron diffraction data [Fig. 1(b)]. Please note that the up and down stand for the directions along and opposite to the internal field. Since the field is staggered, the nominally up direction alternates upon propagation along the a axis. The refinement yields the amplitudes of the m_{xy}^{k1}, m_z^{k1}, m_z^{k2}, and m_z^{k3} Fourier components to be 1.603(4), 0.925(3), 1.719(7), and 0.656(3) μ_B, respectively, at 1.5 K (see also Table S1 of the Supplemental Material [28] for the full Fourier decomposition of the structure as well as the mcif file for its magnetic space group description). The m_{xy}^{k1} component directly represents the size of the in-plane projection of the Nd-moment, whereas the values of the out-of-plane projections are 1.98(1) μ_B for the nominally up and 0.67(1) μ_B for the nominally down directions.

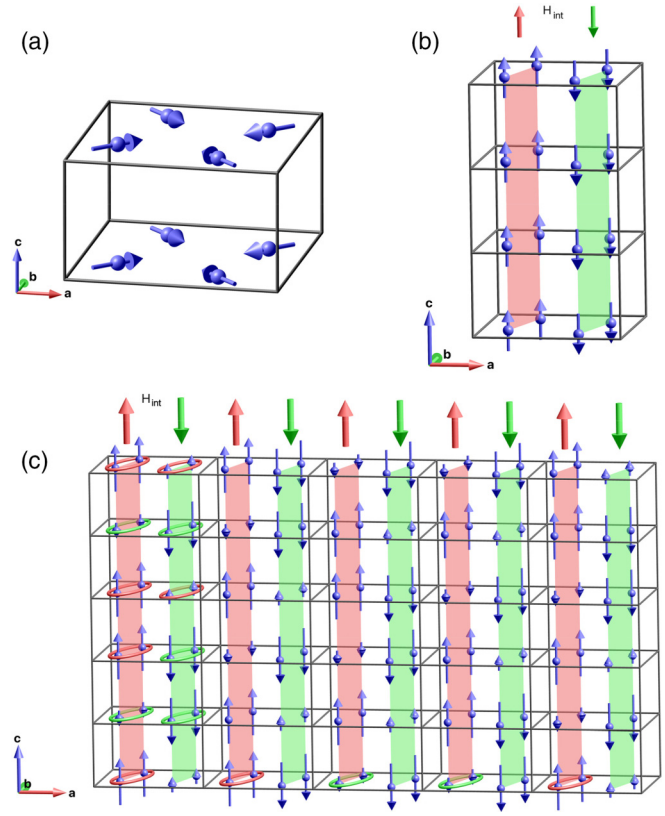

FIG. 2. (a) In-plane (all-in-all-out) Fourier component, m_{xy}^{k1}. (b) Out-of-plane Fourier component, m_z^{k1}, defining the alternating nominally up direction of the internal staggered field, H_{int}. (c) An anharmonic spin density wave consisting of three Fourier components, m_z^{k1}, m_z^{k2}, and m_z^{k3}. The figure was created using *Mag2Pol* [33].

We now discuss a possible mechanism stabilizing this exotic ground state. To do so we propose two main ingredients: (i) a topology of highly anisotropic exchange interactions and (ii) the presence of a nonmagnetic symmetry breaking order parameter (δ^{k1}) which mediates a coupling between the in-plane and the out-of-plane spin configurations. The anisotropic exchange interactions are naturally expected in the case of easy plane magnetic anisotropy with the planes perpendicular to the local twofold axes of the Nd sites with $m.2m$ site symmetry. The easy planes intersect with the ab plane along the [110] and [$\bar{1}$10] directions, and alternate between nearest-neighbor sites forming an orthogonal motif as shown in Fig. 3(a). The experimentally determined magnetic structure with the Nd moments confined within these orthogonal planes strongly indicates this type of magnetic anisotropy. The relevant exchange interactions are defined in Fig. 3(b).

Apart from the J_1 and J_2 exchange parameters typical for 2D SSM, our minimal model also includes a finite in-plane J_3 interaction which couples diagonal Nd sites in the square plaquettes. The orthogonality of the nearest-neighbor easy planes implies a uniaxial exchange anisotropy for the J_1 coupling such that $J_1^x = J_1^y = 0, J_1^z \neq 0$. Considering first the in-plane

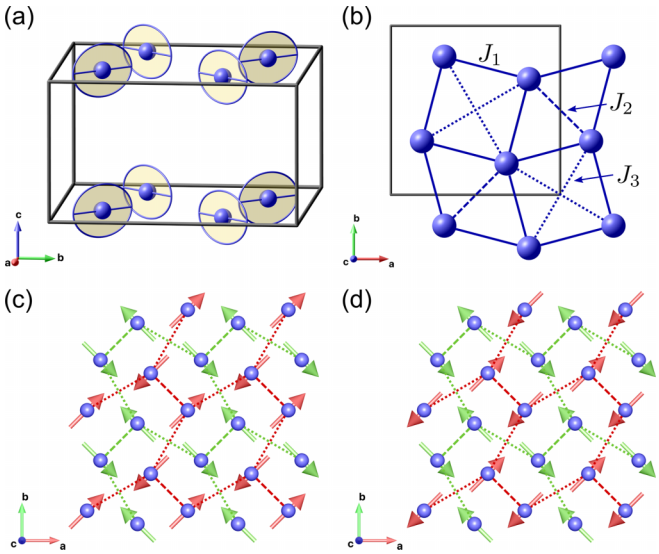

FIG. 3. (a) Easy planes of the four Nd sites in the 4*g* Wyckoff position. (b) Definition of the planar exchange parameters. (c) and (d) Two degenerate configurations of in-plane moments forming the uncorrelated honeycomblike sublattices. The figure was created using *Mag2Pol* [33].

components of the magnetic moments, we decompose the lattice into two orthogonal noninteracting honeycomb-type sublattices [see Figs. 3(c) and 3(d)]. The in-plane moments can be well correlated within the sublattices, but the lack of an exchange interaction between them prevents long range magnetic order (see Sec. 3 of the Supplemental Material [28] for more details and Refs. [34–36] therein). For the out-of-plane moment components, J_1^z is finite and can compete with J_2 as observed in many Shastry-Sutherland systems. Our mean field calculations indicate that depending on the relative strength of the J_1^z, J_2, and J_3 exchange interactions five distinct phases can be stabilized, including an incommensurate order with a propagation vector along the (k_x, k_x) line of symmetry. We restrict our calculations to the 2D case, but the model can be extended to three dimensions by including competing interactions along the c axis, which stabilize the finite value of k_z. In a tetragonal crystal, the above in-plane and out-of-plane instabilities separated on account of the anisotropic exchange interactions do not interact, and their coexistence is not possible in the ground state. The system will choose either the in-plane configuration with the uncorrelated honeycomb sublattices or an ordered state of m_z moments, depending on which yields the lower energy. The presence of structural distortions, however, might change the situation. We did not detect any structural distortions within the resolution limit of our diffraction data measured down to 1.5 K. However, the presence of a "hidden" symmetry breaking order parameter is implied by the temperature dependence of the m_{xy}^{k1} and m_z^{k1} magnetic Fourier components, which have been evaluated by fitting variable temperature powder neutron diffraction data. Both components onset in the high temperature phase at $T_{N1} = 17$ K and persist through all phases down to 1.5 K (see Fig. S2 of the Supplemental Material [28]). The key observation is their substantially different temperature dependences [Figs. 1(c) and 1(d)]. The critical exponent of the all-in-all-out m_{xy}^{k1} component is close to the mean-field value 1/2, while the temperature dependence of the c component m_z^{k1} with ferromagnetic coupling along the b and c axes and antiferromagnetic along the a axis is approximately linear (critical exponent ∼1). A similar result was obtained by Metoki *et al.* [15], who also pointed out that these magnetic modes are transformed by different irreducible representations (irreps) of the paramagnetic $P4/mbm$ space group, excluding bilinear coupling between them. Using the Miller and Love notations for irreps of the crystallographic space groups, as implemented in ISOTROPY [37] and ISODISTORT [38], one can find that m_{xy}^{k1} transforms by the one-dimensional mGM3- irrep, while m_z^{k1} transforms by the 2D mGM5- irrep with order parameter direction $(m, 0)$ in the representation space. Beyond first-order bilinear coupling, analysis of the matrix operators of the mGM3- and mGM5- irreps reveals that there are no higher-order coupling terms between these order parameters. A minimal phenomenological model that can explain the observed critical behavior requires the presence of a nonmagnetic symmetry-breaking order parameter (δ^{k1}) that triggers the onset of long-range magnetic order through a trilinear coupling term with the magnetic order parameters ($\delta^{k1} m_{xy}^{k1} m_z^{k1}$). In this scenario, the m_z^{k1} component is the secondary order parameter induced by a common action of the in-plane m_{xy}^{k1} and the nonmagnetic δ^{k1} order parameters, working together as an internal staggered field along the c axis (H_{int}); the product $\delta^{k1} m_{xy}^{k1} = H_{\text{int}}$ has mGM5-$(m,0)$ symmetry and induces a secondary component of the same symmetry. In this case, the critical exponent of m_z^{k1} is sum of the critical exponents of the magnetic m_{xy}^{k1} and the nonmagnetic δ^{k1} distortions.

The above phenomenology of the high temperature $\mathbf{k}_1 = 0$ magnetic structure describes the situation when the out-of-plane order parameter is secondary to the primary in-plane and nonmagnetic parameters. In other words, the secondary component is induced by H_{int} and it does not necessarily serve to minimize the exchange interactions. The situation, however, is different in the experimentally determined ground state, which consists of coupled in-plane and out-of-plane spin configurations that together optimize the anisotropic exchange interactions. The trilinear coupling term $\delta^{k1} m_{xy}^{k1} m_z^{k1}$ is finite only in the case of long-range magnetic order, and it crucially depends upon the symmetry of the coupled spin configurations, m_{xy}^{k1} and m_z^{k1}. Thus, this term breaks the degeneracy between the uncorrelated honeycomb configurations, choosing the in-plane ordered state with the correct symmetry (m_{xy}^{k1}) to optimize the coupling to m_z^{k1}. The out-of-plane three-up-two-down configuration emerges as a compromise between optimization of the exchange interactions for the out-of-plane moments that give rise to finite k_x and k_z, and the symmetry requirement of the coupling. The latter implies that this configuration must contain the mGM5-$(m,0)$ component. As discussed above, the Fourier decomposition of the anharmonic three-up-two-down spin density wave does indeed contain the m_z^{k1} component with mGM5-$(m,0)$ symmetry. Moreover, this component increases in the ground state, indicating a further optimization of the $\delta^{k1} m_{xy}^{k1} m_z^{k1}$ term. The coupling invariant can also be written in terms of the three-up-two-down magnetic order parameter that is transformed by the

eight-dimensional B2(0,0,0,0,0,0,η_4, η_4^*) irrep associated with the $\mathbf{k}_2 = (1/5, 0, -2/5)$ propagation vector, $\delta^{k1} m_{xy}^{k1}(\eta_4^5 - \eta_4^{*5})$. The general form of this free-energy invariant and the matrix operators used to construct it are provided in Sec. 4 of the Supplemental Material [28] (see also Ref. [39] therein). This free-energy term reveals explicitly the coupled nature of the in-plane mGM3- and the out-of-plane B2 magnetic configurations representing distinct magnetic instabilities in the crystal.

It is interesting that increasing temperature above $T_{N3} = 4.9$ K results in a phase transition where the m_z spin density wave unlocks from the commensurate fivefold periodicity and becomes incommensurate with $\mathbf{k}_{in} = (0.142, 0.142, 0.4)$ while still coexisting with the m_{xy}^{k1} and m_z^{k1} Fourier components. Details of this magnetic structure can be found in the Supplemental Material [28] (Table S2). Apparently, this incommensurate propagation vector minimizes the exchange energy of the out-of-plane moments when they are not compromised by the lock-in condition. This is in full agreement with our mean field calculations, where the incommensurate m_z order is stable in a wide parametric range (see phase diagram in Fig. S5 of the Supplemental Material [28]). The stability of this magnetic structure is also caused by the $H_{\text{int}} m_z^{k1}$ term which is better optimized in this phase than in the high temperature one, containing only the $\mathbf{k}_1 = 0$ components. This is evidenced by the temperature dependence of m_z^{k1} [Fig. 1(d)], which increases in this phase. In other words, one can say that the incommensurate phase has a higher susceptibility to the internal staggered field than the higher temperature $\mathbf{k}_1 = 0$ structure. The intermediate phase is stable only in a narrow temperature range of $T_{N3} = 4.9$ K to $T_{N2} = 6.8$ K in which it optimizes the trilinear coupling term more efficiently than the high temperature phase, but less efficiently than the lock-in ground state.

The above, symmetry-based interpretation of the magnetic structures observed in NdB_4 requires the presence of a nonmagnetic order parameter, δ^{k1}. This order parameter couples distinct magnetic instabilities separated by the anisotropic exchange interactions. We did not observe any signature of the respective symmetry lowering, but the unit cell parameters measured as a function of temperature exhibit a clear anomaly around $T_{N1} = 17$ K, indirectly confirming the onset of structural distortions at this temperature (see Fig. S1 of the Supplemental Material [28]). By analogy with DyB_4 and other systems, Yamauchi *et al.* [14] suggested an electric quadrupole order in NdB_4. Based on the requirement to form the trilinear free energy invariant with the mGM3- and mGM5- order parameters, one can deduce the symmetry of the nonmagnetic distortion, which is GM5+(0,δ). This distortion reduces the crystal structure symmetry down to monoclinic $P2_1/n$. The xy and yz quadrupoles are transformed by the A_2 and B_2 site symmetry representations, respectively, with nonzero subduction frequencies in the space group irrep GM5+. This implies that the quadrupole order satisfies the constraints imposed by the trilinear coupling scheme discussed above and is a likely candidate for the "hidden" order parameter. The monoclinic strains of the magnitude similar to DyB_4 [23] would, however, be reliably detected in our high-resolution backscattering data. Therefore, more precise structural studies are required to directly measure the lattice distortions and unambiguously establish the nature of this order parameter.

In conclusion, the magnetic ground state of NdB_4 represents a unique interplay between strongly anisotropic spins in a frustrated exchange topology and nonmagnetic order parameter. It involves coexisting instabilities coupled via an internal field created by the nonmagnetic distortion, undetectable in the present diffraction data. One instability is the orthogonal all-in-all-out ordering of the in-plane components of the Nd moments. Another instability is a spin density wave of the out-of-plane moments, locked to fivefold periodicity of the lattice to form three-up-two-down sequences in respect of the internal field. These magnetic configurations optimize anisotropic exchange interactions in the system and the coupling term to the nonmagnetic order parameter.

The authors acknowledge financial support from the EPSRC, UK, through Grants No. EP/M028771/1 and No. EP/W00562X/1. This work was also supported by Institut Laue-Langevin and ISIS Neutron and Muon Source (STFC) through the provision of beam time [40].

[1] S. B. Shastry and B. Sutherland, Exact ground state of a quantum mechanical antiferromagnet, Physica B+C **108**, 1069 (1981).

[2] Y. H. Matsuda, N. Abe, S. Takeyama, H. Kageyama, P. Corboz, A. Honecker, S. R. Manmana, G. R. Foltin, K. P. Schmidt, and F. Mila, Magnetization of $SrCu_2(BO_3)_2$ in ultrahigh magnetic fields up to 118 T, Phys. Rev. Lett. **111**, 137204 (2013).

[3] M. E. Zayed, C. Ruegg, J. J. Larrea, A. M. Laeuchli, C. Panagopoulos, S. S. Saxena, M. Ellerby, D. F. McMorrow, T. Strassle, S. Klotz, G. Hamel, R. A. Sadykov, V. Pomjakushin, M. Boehm, M. Jimenez-Ruiz, A. Schneidewind, E. Pomjakushina, M. Stingaciu, K. Conder, and H. M. Ronnow, 4-spin plaquette singlet state in the shastry-sutherland compound $SrCu_2(BO_3)_2$, Nat. Phys. **13**, 962 (2017).

[4] J. Guo, G. Sun, B. Zhao, L. Wang, W. Hong, V. A. Sidorov, N. Ma, Q. Wu, S. Li, Z. Y. Meng, A. W. Sandvik, and L. Sun, Quantum phases of $SrCu_2(BO_3)_2$ from high-pressure thermodynamics, Phys. Rev. Lett. **124**, 206602 (2020).

[5] J. Larrea Jiménez, S. P. G. Crone, E. Fogh, M. E. Zayed, R. Lortz, E. Pomjakushina, K. Conder, A. M. Laeuchli, L. Weber, S. Wessel, A. Honecker, B. Normand, C. Rueegg, P. Corboz, H. M. Ronnow, and F. Mila, A quantum magnetic analogue to the critical point of water, Nature (London) **592**, 370 (2021).

[6] Y. Cui, L. Liu, H. Lin, K.-H. Wu, W. Hong, X. Liu, C. Li, Z. Hu, N. Xi, S. Li, R. Yu, A. W. Sandvik, and W. Yu, Proximate deconfined quantum critical point in $SrCu_2(BO_3)_2$, Science **380**, 1179 (2023).

[7] C. Castelnovo, R. Moessner, and S. L. Sondhi, Magnetic monopoles in spin ice, Nature (London) **451**, 42 (2008).

[8] W. Miiller, L. S. Wu, M. S. Kim, T. Orvis, J. W. Simonson, M. Gamża, D. M. McNally, C. S. Nelson, G. Ehlers, A. Podlesnyak, J. S. Helton, Y. Zhao, Y. Qiu, J. R. D. Copley, J. W. Lynn, I. Zaliznyak, and M. C. Aronson, Magnetic structure of Yb_2Pt_2Pb: Ising moments on the shastry-sutherland lattice, Phys. Rev. B **93**, 104419 (2016).

[9] K. Siemensmeyer, E. Wulf, H.-J. Mikeska, K. Flachbart, S. Gabáni, S. Mat'aš, P. Priputen, A. Efdokimova, and N. Shitsevalova, Fractional magnetization plateaus and magnetic order in the shastry-sutherland magnet TmB_4, Phys. Rev. Lett. **101**, 177201 (2008).

[10] K. Wierschem and P. Sengupta, Columnar antiferromagnetic order and spin supersolid phase on the extended shastry-sutherland lattice, Phys. Rev. Lett. **110**, 207207 (2013).

[11] D. Brunt, G. Balakrishnan, A. R. Wildes, B. Ouladdiaf, N. Qureshi, and O. A. Petrenko, Field-induced magnetic states in holmium tetraboride, Phys. Rev. B **95**, 024410 (2017).

[12] J. Trinh, S. Mitra, C. Panagopoulos, T. Kong, P. C. Canfield, and A. P. Ramirez, Degeneracy of the 1/8 plateau and antiferromagnetic phases in the shastry-sutherland magnet TmB_4, Phys. Rev. Lett. **121**, 167203 (2018).

[13] D. Lançon, V. Scagnoli, U. Staub, O. A. Petrenko, M. Ciomaga Hatnean, E. Canevet, R. Sibille, S. Francoual, J. R. L. Mardegan, K. Beauvois, G. Balakrishnan, L. J. Heyderman, C. Rüegg, and T. Fennell, Evolution of field-induced metastable phases in the shastry-sutherland lattice magnet TmB_4, Phys. Rev. B **102**, 060407(R) (2020).

[14] H. Yamauchi, N. Metoki, R. Watanuki, K. Suzuki, H. Fukazawa, S. Chi, and J. A. Fernandez-Baca, Magnetic structure and quadrupolar order parameter driven by geometrical frustration effect in NdB_4, J. Phys. Soc. Jpn. **86**, 044705 (2017).

[15] N. Metoki, H. Yamauchi, M. Matsuda, J. A. Fernandez-Baca, R. Watanuki, and M. Hagihala, Polarized neutron scattering study of the multiple order parameter system NdB_4, Phys. Rev. B **97**, 174416 (2018).

[16] J. A. Blanco, P. J. Brown, A. Stunault, K. Katsumata, F. Iga, and S. Michimura, Magnetic structure of GdB_4 from spherical neutron polarimetry, Phys. Rev. B **73**, 212411 (2006).

[17] D. Okuyama, T. Matsumura, T. Mouri, N. Ishikawa, K. Ohoyama, H. Hiraka, H. Nakao, K. Iwasa, and Y. Murakami, Competition of magnetic and quadrupolar order parameters in HoB_4, J. Phys. Soc. Jpn. **77**, 044709 (2008).

[18] T. Matsumura, D. Okuyama, T. Mouri, and Y. Murakami, Successive magnetic phase transitions of component orderings in DyB_4, J. Phys. Soc. Jpn. **80**, 074701 (2011).

[19] G. Will and W. Schafer, Neutron diffraction and the magnetic structures of some rare earth diborides and tetraborides, J. Less-Common Met. **67**, 31 (1979).

[20] S. Michimura, A. Shigekawa, F. Iga, T. Takabatake, and K. Ohoyama, Complex magnetic structures of a shastry-sutherland lattice TmB_4 studied by powder neutron diffraction analysis, J. Phys. Soc. Jpn. **78**, 024707 (2009).

[21] R. Watanuki, G. Sato, K. Suzuki, M. Ishihara, T. Yanagisawa, Y. Nemoto, and T. Goto, Geometrical quadrupolar frustration in DyB_4, J. Phys. Soc. Jpn. **74**, 2169 (2005).

[22] S. Ji, C. Song, J. Koo, J. Park, Y. J. Park, K.-B. Lee, S. Lee, J.-G. Park, J. Y. Kim, B. K. Cho, K.-P. Hong, C.-H. Lee, and F. Iga, Resonant x-ray scattering study of quadrupole-strain coupling in DyB_4, Phys. Rev. Lett. **99**, 076401 (2007).

[23] H. Sim, S. Lee, K.-P. Hong, J. Jeong, J. R. Zhang, T. Kamiyama, D. T. Adroja, C. A. Murray, S. P. Thompson, F. Iga, S. Ji, D. Khomskii, and J.-G. Park, Spontaneous structural distortion of the metallic shastry-sutherland system DyB_4 by quadrupole-spin-lattice coupling, Phys. Rev. B **94**, 195128 (2016).

[24] D. Brunt, M. C. Hatnean, O. A. Petrenko, M. R. Lees, and G. Balakrishnan, Single-crystal growth of metallic rare-earth tetraborides by the floating-zone technique, Crystals **9**, 211 (2019).

[25] J. R. Stewart, P. P. Deen, K. H. Andersen, H. Schober, J.-F. Barthélémy, J. M. Hillier, A. P. Murani, T. Hayes, and B. Lindenau, Disordered materials studied using neutron polarization analysis on the multi-detector spectrometer, D7, J. Appl. Crystallogr. **42**, 69 (2009).

[26] L. C. Chapon, M. Pascal, P. G. Radaelli, C. Benson, L. Perrott, S. Ansell, N. J. Rhodes, D. Raspino, D. Duxbury, E. Spill, and J. Norris, Wish: The new powder and single crystal magnetic diffractometer on the second target station, Neutron News **22**, 22 (2011).

[27] J. Rodríguez-Carvajal, Recent advances in magnetic structure determination by neutron powder diffraction, Phys. B: Condens. Matter **192**, 55 (1993).

[28] See Supplemental Material at http://link.aps.org/supplemental/10.1103/PhysRevB.109.L220411 for details of the crystal/magnetic structure refinement and the mean field approach to the ordered states, which includes Refs. [34–36,39].

[29] D. Brunt, G. Balakrishnan, D. Mayoh, M. R. Lees, D. I. Gorbunov, N. Qureshi, and O. A. Petrenko, Magnetisation process in the rare earth tetraborides, NdB_4 and HoB_4, Sci. Rep. **8**, 232 (2018).

[30] R. Ohlendorf, S. Spachmann, L. Fischer, K. Dey, D. Brunt, G. Balakrishnan, O. A. Petrenko, and R. Klingeler, Magnetoelastic coupling and grüneisen scaling in NdB_4, Phys. Rev. B **103**, 104424 (2021).

[31] A. Amorese, D. Khalyavin, K. Kummer, N. B. Brookes, C. Ritter, O. Zaharko, C. B. Larsen, O. Pavlosiuk, A. P. Pikul, D. Kaczorowski, M. Gutmann, A. T. Boothroyd, A. Severing, and D. T. Adroja, Metamagnetism and crystal-field splitting in pseudohexagonal $CeRh_3Si_2$, Phys. Rev. B **105**, 125119 (2022).

[32] D. D. Khalyavin, P. Manuel, M. C. Hatnean, and O. A. Petrenko, Fragile ground state and rigid field-induced structures in the zigzag ladder compound $BaDy_2O_4$, Phys. Rev. B **103**, 134434 (2021).

[33] N. Qureshi, *Mag2Pol*: a program for the analysis of spherical neutron polarimetry, flipping ratio and integrated intensity data, J. Appl. Cryst. **52**, 175 (2019).

[34] M. J. Freiser, Thermal variation of the pitch of helical spin configurations, Phys. Rev. **123**, 2003 (1961).

[35] J. N. Reimers, A. J. Berlinsky, and A. C. Shi, Mean-field approach to magnetic ordering in highly frustrated pyrochlores, Phys. Rev. B **43**, 865 (1991).

[36] D. D. Khalyavin, P. Manuel, J. F. Mitchell, and L. C. Chapon, Spin correlations in the geometrically frustrated $RBaCo_4O_7$

antiferromagnets: Mean-field approach and monte carlo simulations, Phys. Rev. B **82**, 094401 (2010).

[37] H. T. Stokes, D. M. Hatch, and B. J. Campbell, ISOTROPY Software Suite, iso.byu.edu.

[38] B. J. Campbell, H. T. Stokes, D. E. Tanner, and D. M. Hatch, Isodisplace: A web-based tool for exploring structural distortions, J. Appl. Crystallogr. **39**, 607 (2006).

[39] L. Elcoro, B. Bradlyn, Z. Wang, M. G. Vergniory, J. Cano, C. Felser, B. A. Bernevig, D. Orobengoa, G. de la Flor, and M. I. Aroyo, Double crystallographic groups and their representations on the bilbao crystallographic server, J. Appl. Crystallogr. **50**, 1457 (2017).

[40] D. Khalyavin, D. Brunt, N. Qureshi, A. Wildes, B. Ouladdiaf, R. Johnson, G. Balakrishnan, and O. Petrenko, Data set "Neutron diffraction data for magnetic ground state of NdB_4: Interplay between anisotropic exchange interactions and hidden order on a Shastry-Sutherland lattice", Zenodo (2024), doi:10.5281/zenodo.11297311; The data collected at Institut Laue-Langevin can be downloaded from https://doi.ill.fr/10.5291/ILL-DATA.5-41-825 and https://doi.ill.fr/10.5291/ILL-DATA.5-41-871.